The dioctadecylamine monolayer: Textures, phase transitions, and dendritic growth

Ana Flores, Pablo Ize, Salvador Ramos, and Rolando Castillo[a)]
Instituto de Física, UNAM, P.O. Box 20-364, D.F., México 01000

(Received 3 February; accepted 17 June 2003)

The phase diagram of dioctadecylamine Langmuir monolayer has been determined from pressure–area isotherms and from direct observations of the monolayer using Brewster angle microscopy. We describe the observed domains, textures, and phase boundaries for the mesophases presented by this system between 5 °C and 45 °C, at $p\mathrm{H}=3$. The phases were named as G, LE, S_1, and S_2 according to their apparent texture. Contrast between domains of condensed phases is quite low, indicating small tilting of the amine tails. The $G-S_1$, $G-S_2$, $G-\mathrm{LE}$, and $\mathrm{LE}-S_1$ transitions seem to be of first order; meanwhile, the S_1-S_2 transition seems to be of second order. We observed how the froths changed when the area density increases at constant pressure, along the $G-L$, $G-S_1$, and $G-S_2$ phase transitions. In the $L-S_1$ transition, the shape of the domains of the emerging phase is of sixfold dendrites. The phase diagram obtained is very different from those obtained for single chain amphiphiles. In this system, the extent of the phases depends on the acid used to fix the $p\mathrm{H}$. In addition, all our observations indicate that dioctadecylamine does not form a monolayer above $p\mathrm{H}\sim 3.9$. © *2003 American Institute of Physics.* [DOI: 10.1063/1.1598951]

I. INTRODUCTION

Amphiphilic molecules that are nearly insoluble in water can form Langmuir monolayers (LMs) at the air–water interface. The most common way for studying LMs has been through the measurement of the pressure–area isotherms, $\Pi(A,T)=\gamma_0(T)-\gamma(A,T)$, where T is the temperature, A is the area/molecule, γ and γ_0 are the surface tensions of the monolayer and of pure water, respectively. Phase diagrams of LMs have been studied intensively for decades. However, significant advances have been obtained only in the last 10 years due to new experimental techniques. Grazing incidence x-ray diffraction (GIXRD), using intense and highly collimated x rays available from a synchrotron, gives the most explicit information about the monolayer organization.[1] Nevertheless, this kind of experiments is time-consuming and expensive for obtaining an entire phase diagram. Other powerful techniques have been developed to study the monolayer organization, such as polarized fluorescence microscopy (PFM)[2] and Brewster angle microscopy[3,4] (BAM). These techniques complement the information given by GIXRD experiments, because they survey larger scales ($\sim$200 μm) providing information about homogeneity, textures, structure, and dynamics of monolayers.[5–7] These optical techniques are quite sensible for observing very fine details in phase transformations such as molecular tilting. All these new experimental techniques have revealed that singularities in the surface pressure–area isotherms are due to phase changes.[8] Also, they have contributed to obtain a general picture of the structure of the phases of LMs made of fatty acids, long tail alcohols, and in a lesser extent of phospholipids. In these cases, each phase has a different molecular organization,[8] and it has been shown that the molecular organization of condensed phases can be seen as a direct analog of some specific smectic phases.[9] Each phase can be described in terms of four order parameters. These parameters are:[10] (a) positional order; (b) bond or lattice orientational order; (c) tilt order, which is the order of the molecular tilt azimuth with respect to the local orientational order; (d) herringbone order or broken axial symmetry, which is the staggered ordering of the planes of all-*trans* hydrocarbon chains. Furthermore, for these order parameters a distinction has been made between quasilong-range order, in which the order decays accordingly to a power law, and short-range order where the order falls off exponentially with distance.

The degree of understanding of molecular order in the systems mentioned above cannot be extended to other kinds of amphiphilic molecules. This is the case of amines with long aliphatic tails, where a complex behavior has been observed. Primary amine LMs are seriously influenced by the nature of the counter-ions and with the addition of some alcohols to the subphase. Monolayers deposited onto an alkaline water subphase, form carbamates very readily by reaction with atmospheric carbon dioxide. These kinds of behavior have been observed in *n*-octadecylamine, *n*-hexadecylamine, and *n*-docosylamine.[11–13] Docosylamine monolayer has been studied spread on a water surface from $p\mathrm{H}=5$ to $p\mathrm{H}=12.8$ and with several additives.[11,14] Studies on secondary amines are not common in the literature. Although potentially interesting because phases with free rotation of the chains about the long molecular axes should not exist, since the coupling of two tails prevents rotation. The role of translational freedom must also be reduced compared to internal degrees of freedom, due to the lateral motion is hindered because of the two chains. Positions and orientations of head groups can also be involved in ordering, since

[a)]Author to whom correspondence should be addressed. Electronic mail: rolandoc@fisica.unam.mx

interactions among head groups could be laterally anisotropic. Studies on LMs of picrate of dioctadecylamine and of dioctadecylamine have been reported on a water subphase at several pH values, and with subphases containing different types of ions.[15] The difference between the isotherms was attributed to Coulombic repulsion, because of the interplay between the ionized dioctadecylamine and the screening of the ions in the subphase.[15]

In this paper, the phase diagram of dioctadecylamine (DODA) LM has been determined from pressure–area isotherms and from direct observations of the monolayer using BAM. This amine is a secondary amine, with two long aliphatic tails, which is insoluble in water, i.e., the subphase. As far as we know, there are no phase diagrams for secondary amines reported in the literature. In this paper, we describe the observed domains, textures and phase boundaries for the mesophases presented by this LM between 5 °C and 45 °C, at $p\mathrm{H}=3$. The phase diagram obtained is very different from those obtained for single chain amphiphiles.[8,16,17] We found four phases: G, LE, S_1, and S_2, and the phase transitions between these phases were observed. As we will show, DODA does not form a monolayer above $p\mathrm{H}\sim 3.9$, and the extent of the phases depends on the acid used to fix the pH. In the LE–S_1 transition, we observed dendritic crystallization, where domains of the emerging phase form outstanding sixfold dendrites. Here, we present the experimental conditions for obtaining this kind dendritic crystallization. Morphology instability of growing aggregates is one of the subjects that have received a considerable attention in past years. Different growth patterns have been observed, when LMs undergo a first-order phase transition from a fluid to a condensed phase, such as dendritic domains,[18] fractal-like domains,[19] and dense-branched domains.[20]

II. EXPERIMENT

Dioctadecylamine (DODA), $2\mathrm{C}_{18}\mathrm{NH}$, ($\geqslant$99%) was purchased from Fluka Chemie (Switzerland); it was used without any further purification. The amine was spread onto a subphase of ultrapure water (Nanopure-UV, 18.3 MΩ) at several values of pH. The spreading solution was made with chloroform (Aldrich U.S.A., HPLC) at a concentration of 1 mg/ml. HCl (Merck, Mexico) and $\mathrm{H_2SO_4}$ (Merck, Mexico) were used to modify the pH in the acid range and NaOH (Merck, Mexico) in the basic range.

Two Nima LB troughs (models: TKB 2410A and 601 BAM, Nima Technology Ltd., England) were used to obtain the LMs, in both cases a Wilhelmy plate was used to measure the lateral pressure, $\Pi(A,T)$. The trough used to obtain isotherms was isolated from vibrations using a pneumatic tube incorporated into a steel base. The barriers are made of PTFE fitted with stiffening bars defining a working circular area, starting at 1000 cm^2. The trough used for the observations of dendritic domains is a rectangular one, it is made of PTFE with a working area starting at 490 cm^2, and it is isolated from vibrations with a vibration isolation system (model 2S, Halcyonics GmbH, Germany). The speed of compression for obtaining the isotherms was in the order of 50 $\mathrm{cm}^2/\mathrm{min}$ ($\sim$7.2 $\mathrm{Å\,molec^{-1}\,min^{-1}}$) and for observing dendritic domains it was of 25 $\mathrm{cm}^2/\mathrm{min}$ ($\sim$5.3 $\mathrm{Å\,molec^{-1}\,min^{-1}}$). Temperature was kept constant in both cases, with the aid of a water circulator bath (Cole-Parmer 1268-24, U.S.A.). All experiments were carried out in a dust-free environment. The subphase pH was fixed before the development of the isotherms, with a pH-meter calibrated at two points. Our subphase volume is quite large; therefore, the variations of pH are negligible at the end of the experiment.

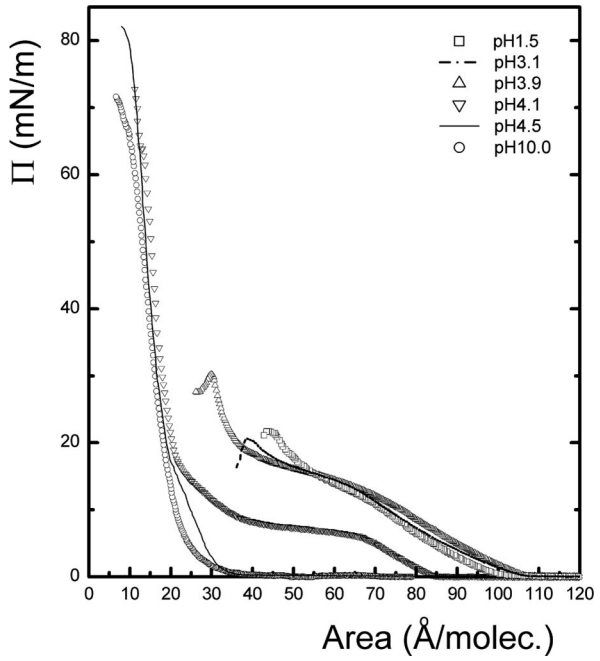

FIG. 1. Isotherms for films made of dioctadecylamine at different values of pH, at 25 °C.

BAM observations during the development of the isotherms were performed in a BAM1 plus (Nanofilm Technologie GmbH, Germany) with a spatial resolution of ≈ 4 μm. The BAM analyzer gave the best contrast while kept at $\sim 0°$ or $\sim 180°$. The experiments for observing the dendritic domains were made with the aid of an Elli2000 imaging ellipsometer (Nanofilm Technologie GmbH, Germany) in the BAM mode (spatial resolution of ≈ 2 μm and 1 μm using the $10\times$ and the $20\times$ objectives, respectively), which allowed us to have the whole field of view in focus due to its movable objective lens.

III. RESULTS AND DISCUSSION

A. Selection of *p*H and isotherms

The behavior of DODA films at the air/water interface depends critically on pH. We present several isotherms for these films in Fig. 1 at 25 °C, and at different pH values. At large pH values ($p\mathrm{H}\geqslant 4.5$), the isotherms are essentially flat, and at area densities of the order of 30 $\mathrm{Å}^2/\mathrm{molec}$ the lateral pressure grows up almost vertically. BAM observations reveal a surface with conglomerates and grains at vanishing lateral pressures that are typical of multilayers [see Fig. 2(a)]. As lateral pressure increases, defects and conglomerates increase too. This behavior changes only as pH is lowered to values ≈ 4.5. Here, there is a narrow transition zone ($p\mathrm{H}\ 4.5-3.9$), where isotherms gradually begin to form a

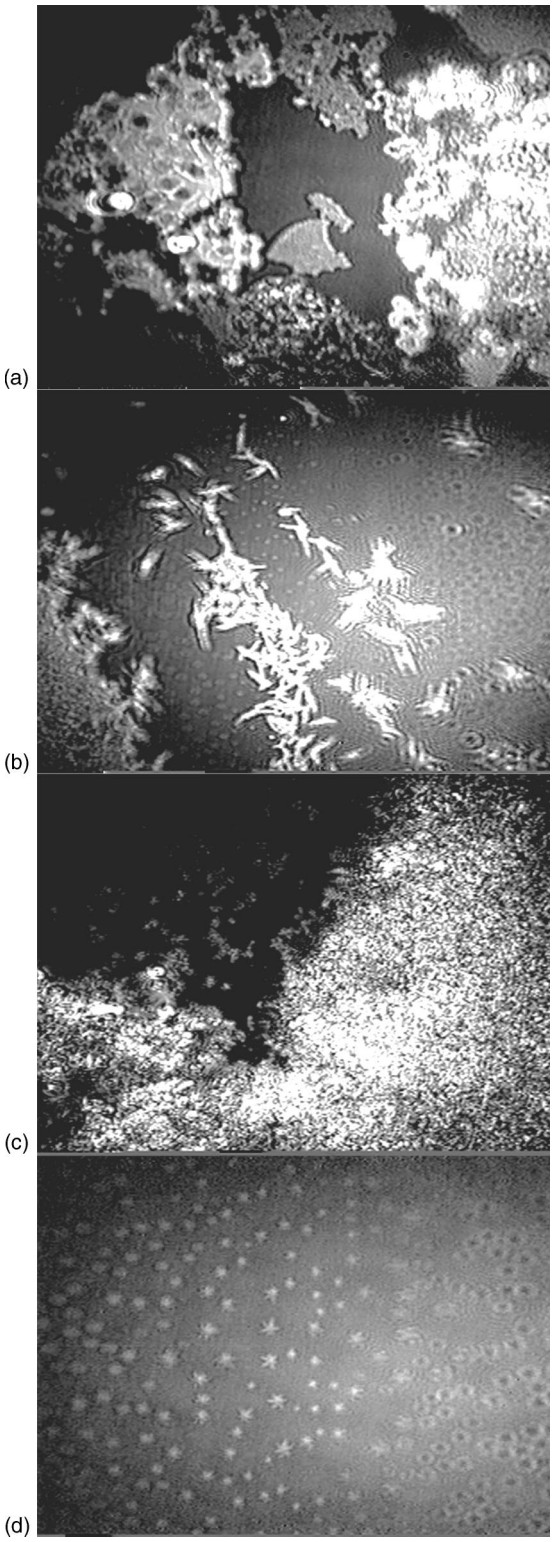

FIG. 2. BAM images for films of dioctadecylamine at different conditions. From top to bottom: (a) pH=10.0, Π=0, and T=25 °C; (b) pH=4.1, Π=7, and T=25.1; (c) pH=4.0, Π=20, and T=25.8 °C; (d) pH=3.1, Π=12.8, and T=22.5 °C. Horizontal full width ~900 μm.

plateau as pH is lowered. A large plateau at $\Pi\sim10$ mN/m can be observed in the isotherm presented in Fig. 1 for pH =4.1. This plateau is quite similar to those observed in a first-order phase transition. However, BAM observations of the film reveal defects and conglomerates typical of a film made of multilayer domains. In Figs. 2(b) and 2(c), we see two examples of BAM observations for the film at pH ~4.1, at different lateral pressures. In some cases, the film seems to be made of small crystal pieces. However, at low lateral pressures, some areas of the film look like the monolayer that will appear at lower pH values. Below pH=3.9, BAM observations reveal a film without any kind of defects, and with several textures depending on temperature and lateral pressure, as it is common in monolayers. In Fig. 2(d), we show an example where a new phase is emerging at $\Pi\sim10$ mN/m and pH=3.1, which will be described below. Isotherms between pH 3.9 and 1.0 show small changes. All seems to indicate that DODA forms monolayers only for pH values below 3.9. Therefore, we decided to use a pH=3.0 subphase in this study.

Many isotherms were made at different temperatures to obtain the phase diagram. In general, monolayers where pH was fixed with sulfuric acid collapsed at larger lateral pressures, in the range of 55–65 mN/m, instead of 20–25 mN/m for those prepared with chlorhidric acid. Features found in the former case most of the times appeared in the later case, but at a few degrees above (~10 °C); just as if the phase diagram was displaced to higher temperatures when H_2SO_4 is used. We do not have a satisfactory explanation for this counterion effect. In Figs. 3 and 4, there are examples of isotherms made at different temperatures for pH=3.0, where pH was fixed with HCl and H_2SO_4, respectively. Isotherms are horizontal at low area densities ($\geqslant$110 Å^2/molec), and they present on compressing big kinks and shoulders that are typical of phase transitions; the compression ends up at collapse.

B. Phases and phase transitions

Figures 5 and 6 show the $\Pi-T$ phase diagrams for DODA LM, when the pH was fixed with HCl and with H_2SO_4, respectively, in the range of temperatures worked in this study (5–45 °C), at pH=3. The coexistence lines were obtained from temperatures and pressures where phase changes occur, as detected in the $\Pi-A$ isotherms and through BAM observation. Most of the times, the phase changes occur before a change of slope in the $\Pi-A$ isotherms (kinks). We found four different phases in the diagrams of Figs. 5 and 6. These phases were named according to the apparent textures observed with BAM, namely, liquid expanded (LE) phase, solid 1 (S_1), and solid 2 (S_2). There is also a region, at very low lateral pressures ($\Pi\leqslant$0.2 mN/m), where condensed phases are in coexistence with the gas phase (G). The monolayer collapses above $\Pi\sim25$ mN/m in Fig. 5 and above $\Pi\sim55$ mN/m in Fig. 6. S_1 phase grows from LE phase as outstanding star-shaped domains or dendritic domains, as we will show below. As far as we now, there are not GIXRD studies for this monolayer. Thus, the actual molecular arrangement of the different phases in the diagrams is not known.

Gas phase is present at very low lateral pressures and always it was found in coexistence with other phases; here, the isotherm is horizontal. At low lateral pressures ($\leqslant$0.2) and at temperatures grater than 14 °C, the $G-$LE coexistence can be more easily observed with BAM, when HCl was used

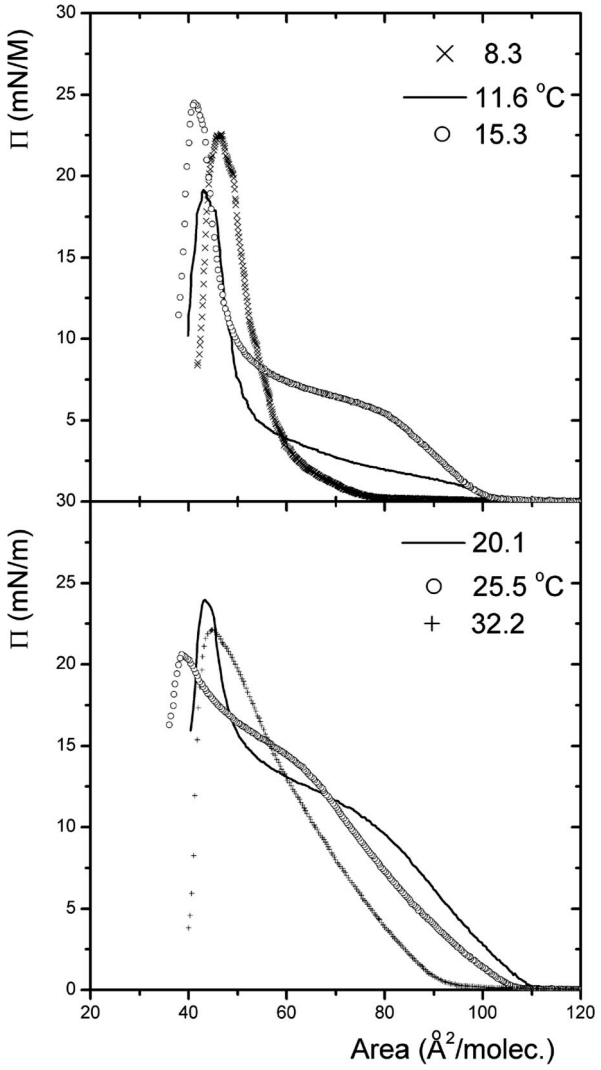

FIG. 3. Isotherms of the dioctadecylamine monolayer at different temperatures (in centigrade scale) and pH=3.0. pH was fixed with HCl.

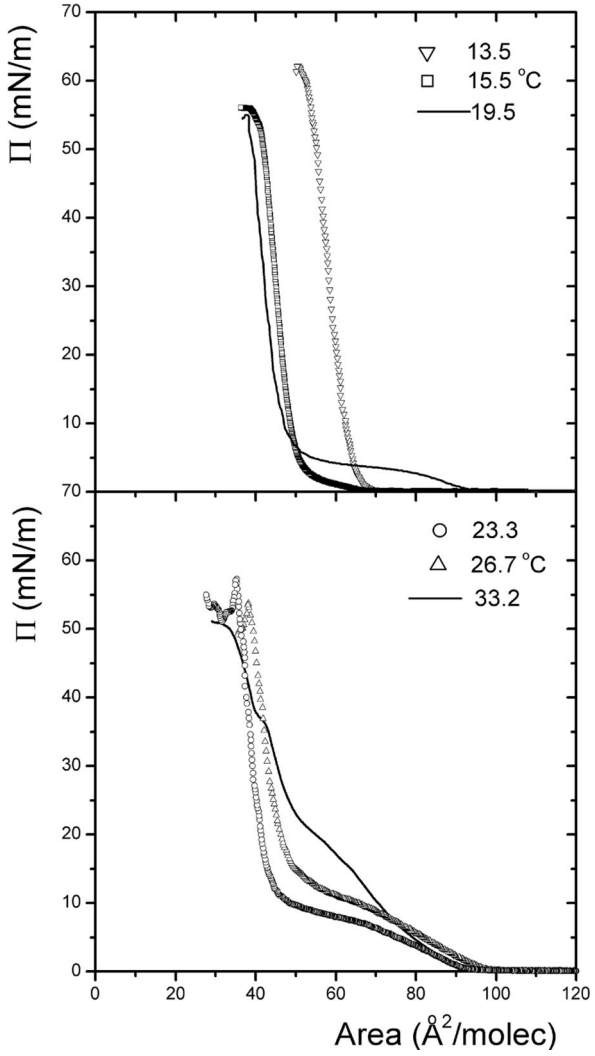

FIG. 4. Isotherms of the dioctadecylamine monolayer at different temperatures (in centigrade scale) and pH=3.0. pH was fixed with H_2SO_4.

to fix the pH, than in the case when H_2SO_4 was used. In Fig. 7, we present several stages from the top to the bottom where the area per molecule is decreasing, at constant lateral pressure and temperature ($T=16.3\,^{\circ}$C and $\Pi\sim0.1$). A 2D foam-like structure with slim walls can be seen at large area per molecule ($a>130\,\text{Å}^2$/molec). As area density is increased, the walls start to be thicker, forming an outstanding polyhedral network. The shape of these bubbles varies along the entire network, but most of the bubbles have six vertices. When density increases even further, the thickening of the walls continues up to the point where the polyhedral network loses the vertices, and the monolayer seems like a layer with holes. The holes become smaller as the area density increases, until the contrastless phase LE is completely formed. These stages seem to illustrate the lever rule in a first-order phase transition. In BAM, it is not as easy as in PFM, to get a binary image[21] where one phase is completely black and the other completely white, to assess the lever rule. This is due to several reasons: BAM images are actually in gray scale, just only a part of the image is in focus, there are diffraction ghosts, etc. In our case, for images in Fig. 7, we measured the fraction in the isotherm tie line vs the area covered by the corresponding phase in the BAM images. The slope of a fitting line was 1.09 with a correlation coefficient of 0.997. In spite of the drawbacks the agreement is good. The same kind of events is observed in the coexistence $G-S_2$ (see Fig. 8) at low lateral pressures ($\leqslant 0.2$) and at temperatures below $\sim 9\,^{\circ}$C, for the case when pH was fixed by HCl. However, in this case the network is quite different from that observed in the $G-$LE. In the $G-S_2$, we do not observe a polyhedral structure. Instead, we can observe long and irregular filaments of S_2 phase, that increase in number as area density increases [see Fig. 8(c)], up to a point were the contrast is lost, i.e., when the phase transition has ended up. This kind of structures has been observed in another amine, stearylamine,[22,23] using PFM at low pH. Domain shapes have been explained by two competing effects: the line tension of the 1D interface between the coexisting phases, and the electrostatic repulsion between the polar head groups of the amphiphiles.[24,25] $G-S_1$ coexistence is always a coexistence of irregular dots of S_1 phase and the gas phase.

LE phase is found in a temperature range of 14–35 °C

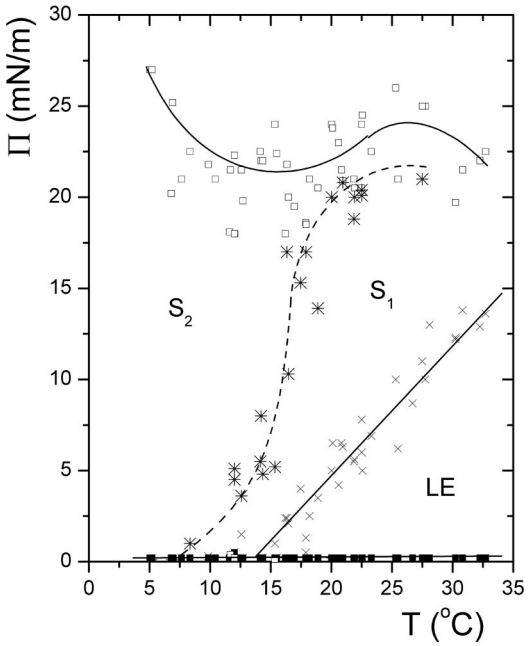

FIG. 5. Surface pressure–temperature phase diagram for dioctadecylamine. The phase changes were obtained from the Π–*A* isotherms (□,■) and from BAM observations (×,∗). *p*H was fixed with HCl.

and at lateral pressures ~0.2–15 mN/m, when *p*H is fixed with HCl. In the case of H_2SO_4, this transition is displaced to higher temperatures, in the range of 22–45 °C, and at higher lateral pressures ~0.2–30 mN/m. This phase does not

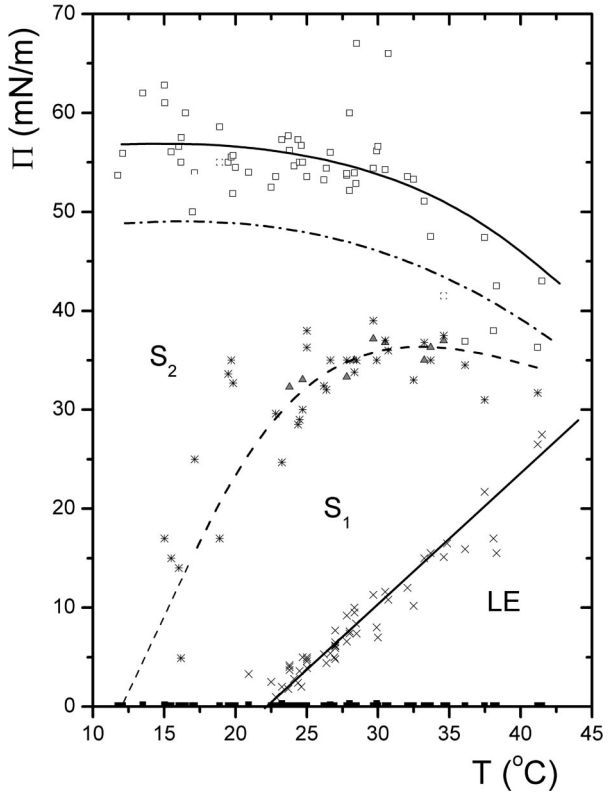

FIG. 6. Surface pressure–temperature phase diagram for dioctadecylamine. The phase changes were obtained from the Π–*A* isotherms (□,▲,■) and from BAM observations (×,∗). *p*H was fixed with H_2SO_4.

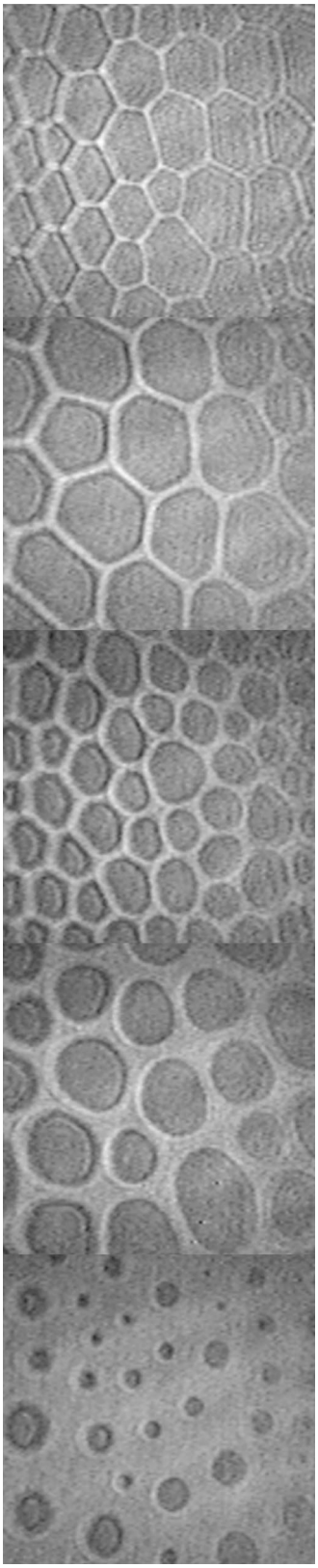

FIG. 7. Sequence of BAM images showing the *G*–LE phase transition ($T = 16.3$ °C and Π~0.1, *p*H fixed with HCl). Starting from the top image, most of the monolayer is *G* phase. Close to the end of the phase transition, the bottom image most of the monolayer is the LE phase. Horizontal full width ~360 μm.

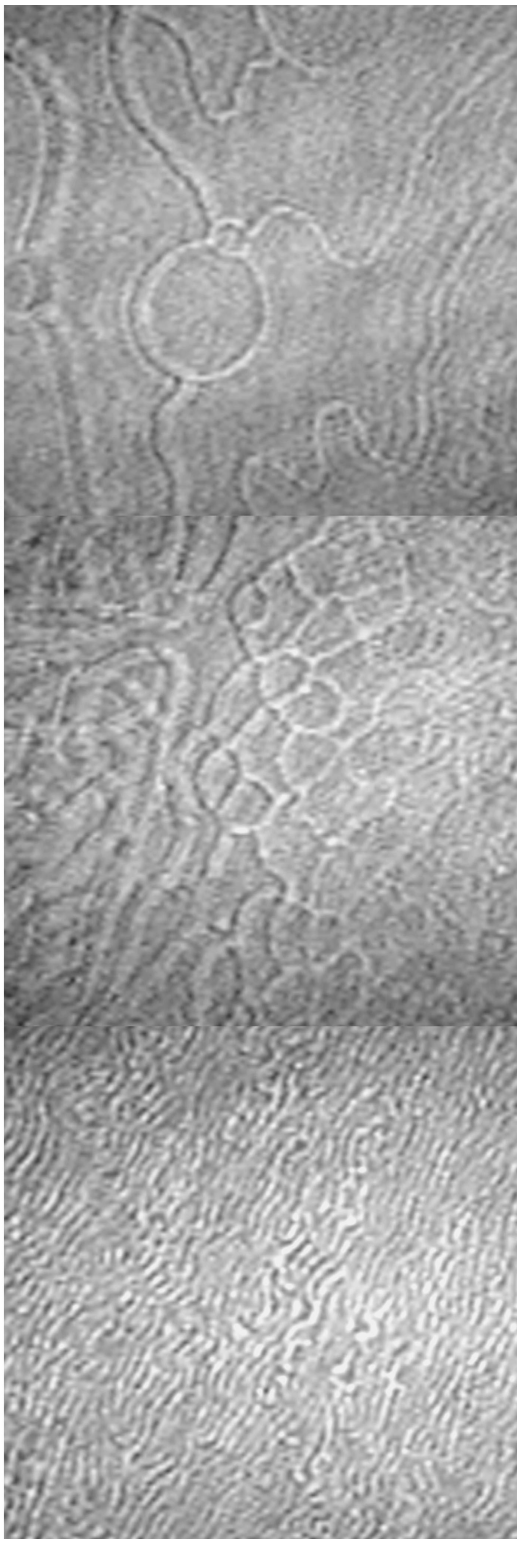

FIG. 8. Sequence of BAM images showing the $G-S_2$ phase transition ($T=6.8\,^{\circ}\mathrm{C}$ and $\Pi\sim0.1$, pH fixed with HCl). At the top image (a) most of the monolayer is in G phase. In bottom image (c) most of the monolayer is in S_2 phase. Horizontal full width $\sim360\ \mu$m.

present any kind of domains or shades of gray when observed with BAM; it is optically isotropic. Defects show that the monolayer is not rigid; the relative positions of defects do not change easily. Therefore, LE phase behaves as liquid phase, although not very fluid. In LE phase, molecules should be not far apart from each other ($\sim$9–10 Å), since typical area density values for this phase are around 80–100 Å^2/molec; correlation between the tails of these molecules should be of short range.

At higher lateral pressures, the monolayer in LE phase reaches a phase transition. Here, small light-gray dot domains of S_1 phase, randomly distributed in the contrastless dark-gray liquid phase, suddenly appear in the BAM images of the monolayer. At the very beginning, the dot domains seem to be round at the microscope resolution. However, as far as the compression goes on, the dot domains grow up in a form of outstanding six-leg star shaped domains; all apparently with the same shade of gray. During the growth of star domains, apparently no new dot domains are formed. If pressure decreases, dot and star domains disappear and they reappear as pressure increases again. In Figs. 9 and 10, we present an example of the observed events with BAM as pressure increases in the monolayer during the course of $\Pi-A$ isotherm determinations, when HCl was used to fix the pH. As the lateral pressure increases, the legs of the star domains grow up as dendrites [see Fig. 9(c)]; we will show it in detail below. Because of compression, star domains grow, become closer to each other, until they are distorted [see Fig. 9(d)]. If the analyzer of the microscope is rotated, there is an angle where the light gray hue of dot and star domains can be exchanged with the dark hue of the contrastless layer [see Fig. 9(e)]; this angle does not depend on the orientation of star domains. This test reveals that the reflectivity of the monolayer is related to the tilting characteristic of the phases and not to multilayering. After the growing and the distortion of domains, they join together, roughly covering all the monolayer until the legs of the star domains (dendrites) amalgamate and fade away slowly (see Fig. 10). Most of the times, these events coincide with the shoulder of the isotherms, which appear $\approx$60–70 Å^2/molec. We will come back to this issue below. The texture of the S_1 phase seems like a speckled surface with irregularly shaped domains with different shades of gray. This phase is quite rigid; it seems to be like a solid phase. Some of the small bright domains are remains of the dendritic domains. As the pressure increases the size of the domains decreases, although, they remain irregular and some contrast is lost [see Fig. 10(c)]. The LE$-S_1$ transition is reversible for cycles of compression and decompression, and they present hysteresis. Therefore, all seems to indicate that the LE$-S_1$ is a first-order phase transition. Linear fitting of the coexistence line [$\Pi(\mathrm{mN/m})=1.26T(\mathrm{K})-370.97$] allows us to obtain the 2D Clausius–Clapeyron equation. Our $d\Pi/dT$ is close to value obtained for other two-tail amphiphile monolayers, as DMPC (2.35 mN/m K^{-1}),[26] DMPA (1.05 mN/m K^{-1}),[26] and DPPC (1.42 mN/m K^{-1}).[27] The latent heat of transition for the LE$-S_1$ transition at 23 °C, is $l=89.86$ KJ/mol, which is of the same order of the two-tail DPPC monolayer (114 KJ/mol) (Ref. 27) at 20 °C.

S_2 phase is located above the S_1 in the $\Pi-A$ phase diagram. S_2 is contrastless using BAM, and it is apparently quite rigid; so it seems to be a solid phase. The S_1-S_2 phase transition is detected most of the times only with BAM, when the contrast is lost as pressure increases. However, the

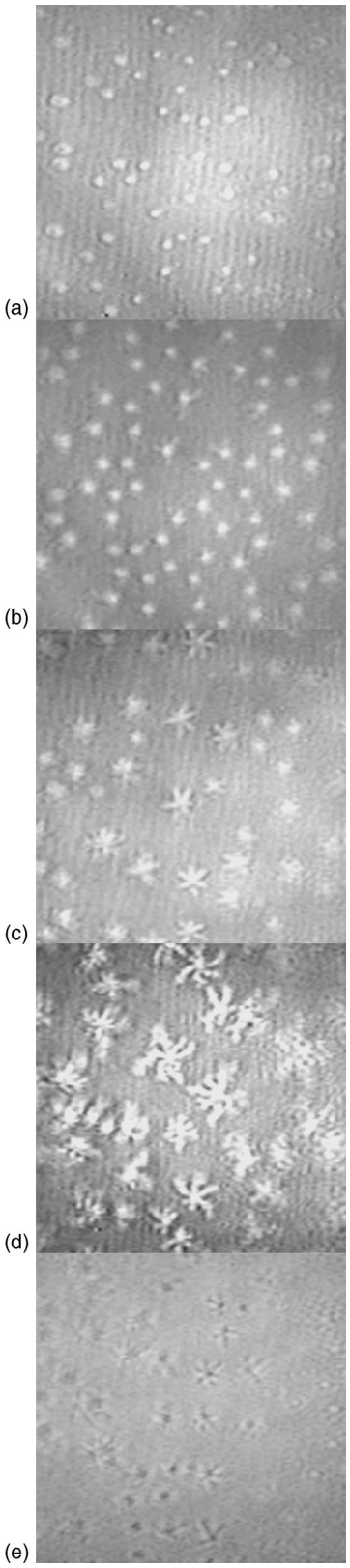

FIG. 9. BAM images for the LE–S_1 phase transition at 25.5 °C. The images were obtained at different lateral pressures, from the top to the bottom (a) $\Pi=7.2$; (b) $\Pi=7.5$; (c) $\Pi=8.3$; (d) $\Pi=12$; all in mN/m. In the lowest panel, an image of star domains where the bright and dark areas are inverted, because the analyzer of the Brewster angle microscope has been rotated. Horizontal full width 360 μm.

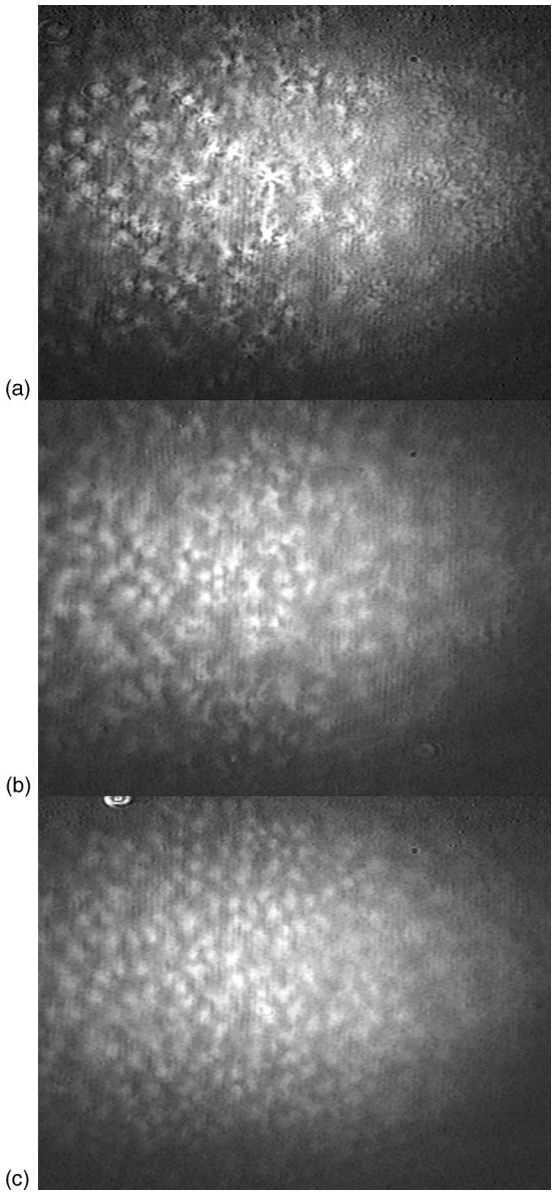

FIG. 10. Speckled surface with irregularly shaped domains characteristic of S_1 phase, as observed with BAM. (a) Distorted star domains at $T=21.9$ °C and $\Pi\sim11.5$ mN/m; (b) amalgamated star domains at a pressure slightly above than given in (a); (c) texture of S_1 phase at $\Pi=12$ mN/m and $T=25.5$ °C. Horizontal full width 900 μm.

contrast fades away continuously, suggesting that transition is a second-order phase transition. This makes the localization of the S_1-S_2 border very difficult and not precise, for this reason, we indicated the border as a dotted line in Figs. 5 and 6. However, the transition is reversible. S_2 phase presents big areas almost with the same shade of gray. In this phase, the amine molecules are quite close ($\sim$7 Å), since the area density is $\approx$45–60 Å^2/molec. If some analogy with fatty acids can be made, probably in this S_2 phase the tails are fully stretched (all-*trans*) and without tilting to be optically isotropic. On compressing S_2 phase, the monolayer collapses at area densities of the order of 35–50 Å^2/molec. However, there are two events to be mentioned. In some of the compressions made to obtain the phase diagram, before decollapse ($\sim$3–5 mN/m) there is a small kink, although, nothing

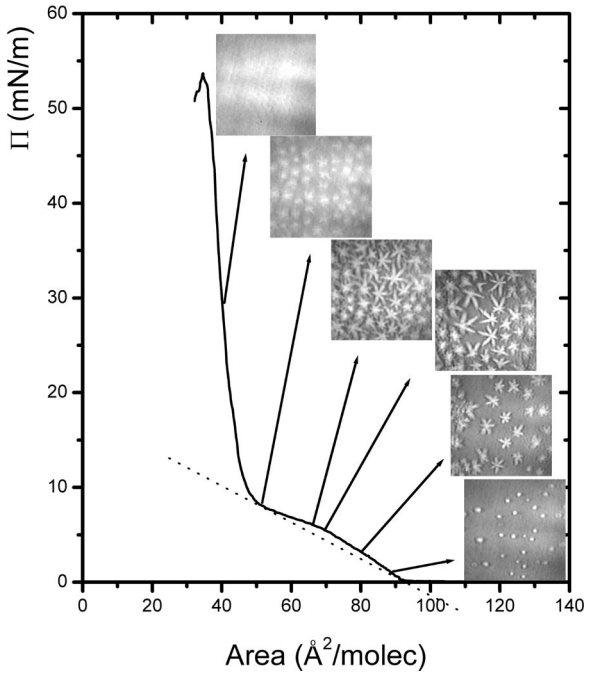

FIG. 11. BAM observations of the dioctadecylamine monolayer along the course of a normal compression to obtain an isotherm (compression rate 50 $cm^2\,min^{-1}$~7.2 Å $molec^{-1}\,min^{-1}$). The dotted line is an aid to the eye to see the wide shoulder in the isotherm.

was observed with BAM. In other cases, we observed a network almost invisible developing in the contrastless S_1 phase. Sometimes this observation coincides with the kink, but most of the times it occurs around 10 mN/m below the collapse. The low contrast, the steepness of the isotherm, and the proximity to the collapse made impossible to study this not quite repeatable change. It is not clear to us, if these events correspond to some kind of precollapse. For this reason, we marked a dotted–dashed line before the collapse for the case of monolayers prepared with sulfuric acid (Fig. 6).

C. Dendritic domains

At the LE–S_1 coexistence line, the transition starts on with the formation of light gray dot domains, which grow up as six-leg star shaped domains (dendrites) as far as pressure increases at constant temperature. The growing up of these star domains is quite slow, compared to the time of compression. Even at the smallest compression rate used here, the transition occurs, but not at constant pressure. Therefore, a small overpressure is produced in the system before the star domains invade all the monolayer. This overpressure is not big at low temperatures, but it can reach values ≈5–7 mN/m at 30–40 °C. Consequently, since the system is not in thermal equilibrium, the isotherms are not horizontal along this transition; probably we are coming into a metastable region (supercooled liquid). In Fig. 11, we present an isotherm and the structures observed in the monolayer with BAM, along a normal compression. Taking into account this behavior, it is now clear why the LE–S_1 phase transition was determined mainly using BAM instead of isotherms for determining the phase diagrams of Figs. 5 and 6.

We prepared monolayers with LE and S_1 phases coexisting, and maintaining the lateral pressure constant with the aid of the servomechanism of the trough, we observed the monolayer for a long time; the area lost in these experiments was quite low in the range of ~7%. We reached the constant lateral pressure compressing the monolayer at lower compression rates than those used for obtaining the isotherms presented above. In these experiments, we tried to maintain the air above the subphase at a temperature at most 1 °C below the subphase temperature. In these experiments, we observed that star domains grew up quite slowly (in the range of hours) and that they were in fact sixfold dendrites. Figure 12 shows an example of dendritic crystallization at constant pressure and temperature, where different areas of the monolayer are observed as time elapses. We do not think that these dendritic patterns are formed due to DODA impurities. If impurities were responsible for this form of growing, they would grow at larger speed, in the range of half a minute, and they would form fractal structures, as it has been observed in other systems.[19] In denditric growth regime, the growth direction is correlated to crystallographic direction of the lattice, due to the line tension anisotropy. Therefore, the six-leg star dendrites, with an angle of 60° on the average between adjacent dendritic legs, are a consequence of an almost certainly hexagonal lattice. The weak tilt indicated by the low anisotropy contrast found with BAM probably plays a minor role in main growth direction, in agreement with what is found in systems with strongly tilted aliphatic chains.[28] In addition, it is clear from our observations, that when a star domain does not have a neighbor star domain in some specific direction, the dendritic crystallization growth will produce a larger dendritic leg in that direction. In mature star domains [see Fig. 12(d)], it is possible to see that the legs have a slight different shade of gray, revealing a small difference in tilting of the diamine tails in the dendritic legs of the star domains. The contrast between domains comes from different tilting of the hydrocarbon tails. This contrast is stronger in correlated tilted phases. Each shade of gray corresponds to a different azimuth tilt direction in a domain. We also observed the monolayer as pressure relaxed when LE and S_1 phases were coexisting. Typically, pressure drop was slow (~in 10 min, Π lowered ~1 mN/m), and depending on overpressure dendritic stars stayed for a long time. The size of dendrites decreases as time elapses, until the small round domains are reached.

One interpretation of our results is that the 2D disks of S_1 phase are growing in a supercooled liquid matrix showing a fingering instability similar to those observed in 3D. In 3D, fingering morphologies are due to either the production of latent heat at the moving interface or to the expulsion of chemical impurities from the solid phase at the interface.[29–31] Diffusion of either the excess heat or excess impurities away from the interface proceeds more efficiently for a modulated interface, through what is called the Mullins–Sekerka instability. Studies of morphology of growing phases in LMs are normally based on PFM that requires the use of dyes.[19] However, the heat build-up at the interface has been ruled out in our community, since LMs rest on a large body of water interface that acts an isothermal reservoir, and the heat liber-

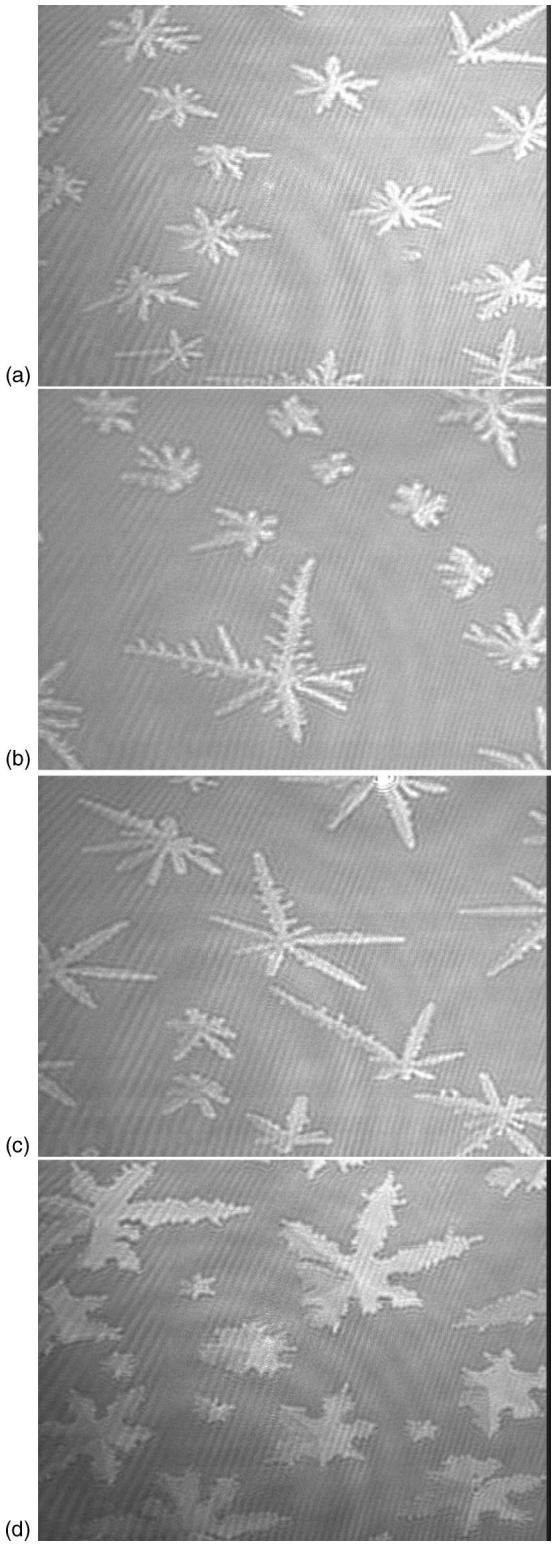

FIG. 12. BAM images of the monolayer with LE and S_1 phases coexisting, as a function of elapsed time, maintaining the lateral pressure constant ($\Pi = 7.5$ mN/m). From top (a) to bottom (d): 1 min, 7 min, 12 min, and 72 min after fixing pressure. ($T = 22.4\,^{\circ}$C, rate of compression before fixing pressure 4.1 Å molec^{-1} min^{-1}, lost of area after 72 min~7%, *p*H fixed with sulfuric acid, and air above the subphase was at a temperature at most 0.8 °C below the subphase temperature.) Horizontal full width is 220 μm.

ated is very low (1.49×10^{-19} J/molec). In LMs, we have a 3D system taking into account the subface, where molecules forming the monolayer are the only ones, which are restricted to move in 2D. Quite recently, a hydrodynamic mechanism has been proposed,[32] based on Marangoni flow, which describes the growth instabilities of liquid-condensed islands in the supercooled liquid-expanded phase. This Marangoni instability seems to be intrinsic to LMs and it is not controlled by the expulsion of chemical impurities from the liquid condensed phase. The hydrodynamic transport of the insoluble surfactants seems to overwhelm the passive diffusion and to provide a mechanism for fingering instabilities. A study to determine the growth mechanism producing the dendritic domains in the monolayer of interest here is underway. Here, both the curvature of the leg tips of the dendrites as a function of the leg length, and the arm modulation are measured. Our results will be published later.

In summary, we have obtained the phase diagram of an amine LM with two long aliphatic tails. This system is peculiar because it forms LM only in a limited range of *p*H, and its phase diagram is very different from those obtained for single chain amphiphiles, such as fatty acids, esters, alcohols, etc., or from two-chain phospholipids. We did not find a mosaic of irregular shaped domains as rich as those obtained for single chain amphiphiles, due to the different azimuthal tilt directions of the all-*trans* hydrocarbon tails. In our case, even the contrast between domains of different phases is low, although, clearly visible. We found four phases, although more phases could be undetected because of the low order in this LM due to the disorder introduced by the aliphatic tails that cannot align parallel near the interconnecting nitrogen. This system also presents an outstanding dendritic crystallization; as in other cases, it is not clear the origin of these growth instabilities.

ACKNOWLEDGMENTS

We acknowledge the partial support of CONACYT and DGAPAUNAM grants (36680-E and IN-113601).

[1] J. Als-Nielsen, D. Jacquemain, K. Kjaer, F. Leveiller, M. Lahav, and L. Leiserowitz, Phys. Rep. **246**, 251 (1994).
[2] C. M. Knobler, in *Advances in Chemical Physics*, edited by I. Prigogine and S. A. Rice (Wiley, New York, 1990), Vol. LXXVII, p. 397.
[3] D. Höning and D. Möbius, J. Phys. Chem. **95**, 4590 (1991).
[4] S. Henon and J. Meunier, Rev. Sci. Instrum. **62**, 936 (1991).
[5] G. A. Overbeck and D. Mȍbius, J. Phys. Chem. **97**, 7999 (1993).
[6] D. K. Schwartz, M. W. Tsao, and C. M. Knobler, J. Chem. Phys. **101**, 8258 (1994).
[7] Th. M. Fischer, R. F. Bruinsma, and C. M. Knobler, Phys. Rev. E **50**, 413 (1994).
[8] V. M. Kaganer, H. Möhwald, and P. Dutta, Rev. Mod. Phys. **71**, 779 (1999).
[9] A. M. Bibo, C. M. Knobler, and I. R. Peterson, J. Phys. Chem. **95**, 5591 (1991).
[10] D. Andelman, F. Brochard, C. M. Knobler, and F. Rondelez, in *Micelles, Membranes, Microemulsions, and Monolayers*, edited by W. M. Gelbart, A. Ben-Sahul, and D. Roux (Springer, New York, 1994), p. 559.
[11] G. L. Gaines, Nature (London) **298**, 544 (1982).
[12] P. Ganguly, D. V. Paranjape, and F. Rondelez, Langmuir **13**, 5433 (1997).
[13] P. Ganguly, D. V. Paranjape, K. R. Patil, M. Sastry, and F. Rondelez, Langmuir **13**, 5440 (1997).
[14] M. Bardosova, R. H. Tredgold, and Z. Ali-Adib, Langmuir **11**, 1273 (1995).
[15] E. Brynda, I. Kmínek, and S. Nešpůrek, J. Mater. Sci. **24**, 4164 (1989).
[16] S. Ramos and R. Castillo, J. Chem. Phys. **110**, 7021 (1999).

[17] S. Riviere, S. Henon, J. Meunier, D. K. Schwartz, M. W. Tsao, and C. M. Knobler, J. Chem. Phys. **101**, 10045 (1994).
[18] K. I. Iimura, Y. Yamauchi, Y. Tsuchiya, T. Kato, and M. Suzuki, Langmuir **17**, 4602 (2001).
[19] A. Miller and H. Möhwald, J. Chem. Phys. **86**, 4258 (1987).
[20] G. Wiedemann and D. Vollhardt, Langmuir **13**, 1623 (1997).
[21] B. G. Moore, C. M. Knobler, S. Akamatsu, and F. Rondelez, J. Phys. Chem. **94**, 4588 (1990).
[22] K. J. Stine and D. T. Stratmann, Langmuir **8**, 2509 (1992).
[23] K. J. Stine, M. F. Bono, and J. Scott Kretzer, J. Colloid Interface Sci. **162**, 320 (1994).
[24] H. M. McConnell, Annu. Rev. Phys. Chem. **42**, 171 (1991).
[25] M. Seul and D. Andelman, Science **267**, 476 (1995).
[26] O. Albrecht, H. Gruler, and E. Sackmann, J. Phys. (Paris) **39**, 301 (1978).
[27] N. Krasteva, D. Vollhardt, G. Brezesinski, and H. Möhwald, Langmuir **17**, 1209 (2001).
[28] U. Gehlert and D. Vollhardt, Langmuir **13**, 277 (1997).
[29] J. S. Langer, Rev. Mod. Phys. **52**, 1 (1980).
[30] H. C. Fogedby, E. Schwartz Sorensen, and O. G. Mouritsen, J. Chem. Phys. **87**, 6706 (1987).
[31] O. G. Mouritsen, Int. J. Mod. Phys. B **4**, 1925 (1990).
[32] R. Bruinsma, F. Rondelez, and A. Levine, Eur. Phys. J. E **6**, 191 (2001).